

## Response to reviewers - Minor revisions for manuscript EGUSPHERE-2022-770

We wish to thank the editor and referees for useful comments on our work. In the following we report a point-by-point response to the comments (in blue).

The supplementary material code that was included as a .zip file with our original submission has now been moved to a dedicated Zenodo repository (<https://zenodo.org/record/7720281#%23.ZAvnArTMlpN> ) Referred to in the manuscript and listed in the online assets.

### Referee # 1

Thank the authors for their efforts to resolve my comments. I just have some minor comments for the figures:

1. Add the units for the x/y labels of latitude and longitude
2. Add the numbering for the sub-figures

We thank the reviewer for the attention devoted to our work. In the revised manuscript we have added latitude and longitude units to the map labels. We have also added numbering for the sub-plots of all figures with multiple sub-plots where this was missing (except in Figure 6 and 7, in which sub-figures already have row and column labels).

### Referee # 2

I would like to thank the authors for the additional effort they put in the revision of the manuscript. Please find below some additional final remarks (line numbers refer to the revised manuscript with marked changes):

We thank the reviewer for the attention devoted to the manuscript.

**Title:** the model version changed from 4.2 to 4.1 – is that correct (i.e. intended)?

Yes, this is intended, as stated in our response to the previous round of reviews. Thank you for pointing this out. The methodology developed here can be applied to both model versions, but ESM 4.1 is the published version of reference (Dunne et al., 2020, cited in the paper) and the title of the manuscript now reflects the correct published model version. The LM4.2 is the version currently under active development at GFDL in but not the published reference version for this work.

**L186:** I would remove the reference to Zakšek et al. (2011). They define the sky view factor simply as the fraction of the visible sky – in contrast to studies like Dozier and Frew (1990) and Helbig et al. (2009), which apply the correct definition of the sky view factor for radiation purposes.

We agree and remove the citation.

**L196:** I'm still a bit puzzled by the approximation of the terrain configuration factor. Wouldn't the simple approximation  $C_t = 1.0 - V_d$  be more accurate?

According to Dozier and Frew (1990), page 965, for given S local slope:

$$C_t = \frac{1}{\pi} \int_0^{2\pi} \int_{H_\phi}^{\psi_\phi} \eta_\nu(\theta, \phi) \sin \theta [\cos \theta \cos S + \sin \theta \sin S \cos(\phi - A)] d\theta d\phi \quad (9a)$$

$$C_t = \frac{1 + \cos(S)}{2} - V_d \quad (9b)$$

*“Rigorous calculation of  $C_t$  is difficult because it is necessary to consider every terrain facet visible from a point to calculate  $\eta_\nu$  [the anisotropy coefficient]. In contrast to the sky radiation, the isotropic assumption is unrealistic because considerable anisotropy results from geometric effects, even if the surrounding terrain is a Lambertian reflector or a blackbody emitter. We therefore note that  $V_d$  for an infinitely long slope is  $(1 + \cos(S))/2$ , which leads to the approximation in (9b).”*

The calculation proposed by Dozier and Frew 1990 which yields eq. the approximation (9b) reported here is obtained by integrating eq. (9a) between the horizon and the tangent to the local slope. The relation  $C_t = 1.0 - V_d$  is obtained from eq. (9b) if one then further assumes that the surface is locally flat, i.e.,  $\cos(S)=1$ . Therefore, we believe it is adequate to use eq. (9b) in this application.

**L203:** I would explicitly state that the solar incidence angle is measured relative to the normal of the **horizontal** surface.

This information is reported at line 192 of the revised manuscript:

*“Here  $\mu_i$  is the cosine of the solar incidence angle (i.e., angle between the incoming direct light beam and the normal to the land surface) while  $\mu_0$  is the cosine of the solar zenith angle (i.e., the incidence angle with respect to a horizontal plane).”*

**L497:** “can be in principle be applied” to “can in principle be applied”

Amended.

**L549:** I agree that a higher sub-grid tile structure would only be needed in areas with complex terrain. However, would the current model architecture be able to handle such an “unbalanced workload”? For instance: one computer cluster node would have to process a domain slice with complex terrain, while another one would process a domain slice with flat terrain. Would the former node not simply slow down the latter and thus determine overall run time? Or is your model able to distribute such an unbalanced workload evenly?

This is indeed a well-understood load imbalance issue, and the infrastructure used for running the GFDL ESM is already geared toward solving such problem. We have added the following clarification in the manuscript:

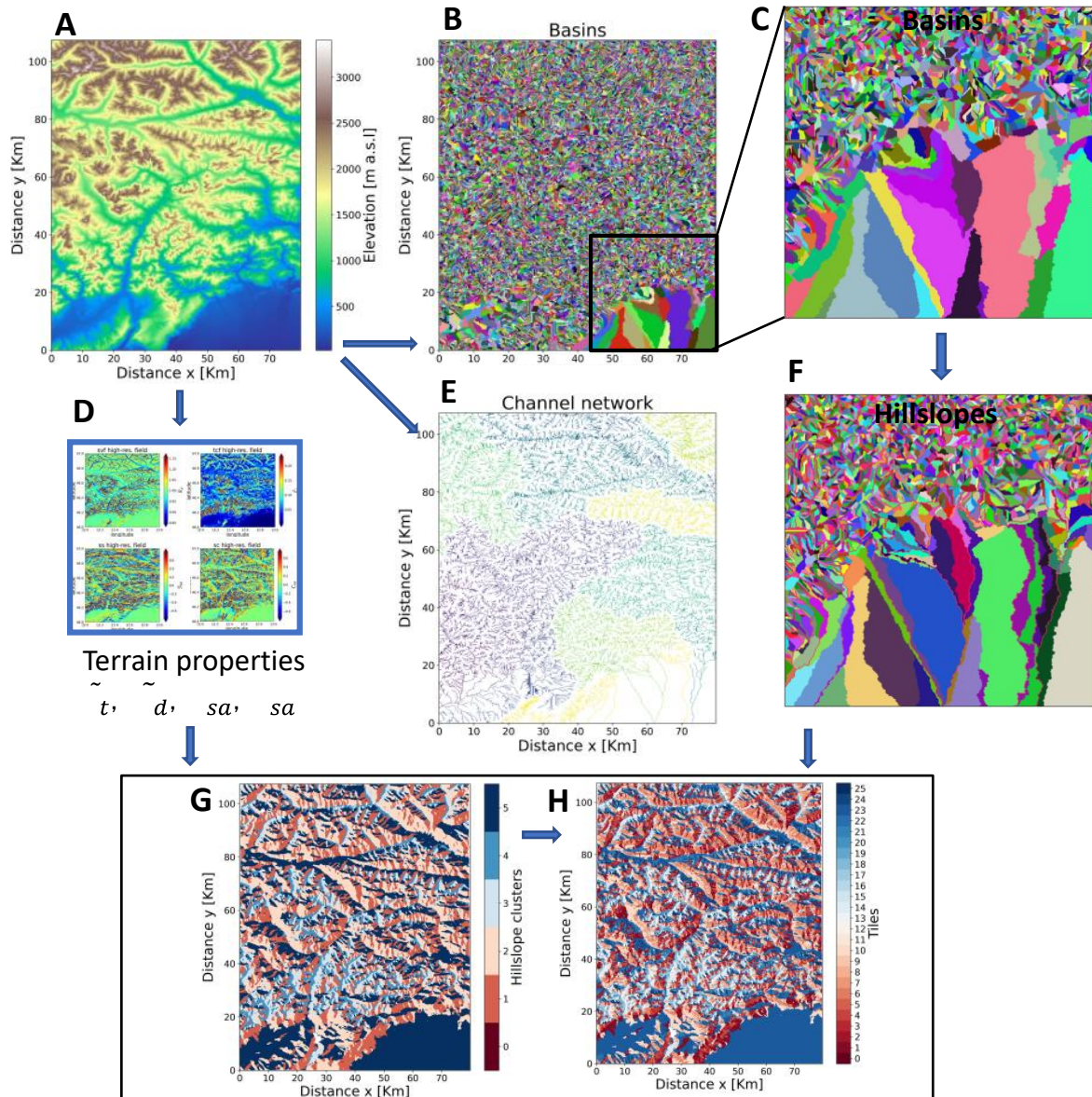
*“We note that in the case of the GFDL ESM, the model infrastructure is already suited for grids of this type, which can be characterized by an uneven number of sub--grid units in different grid cells depending on the local terrain properties. On the model start, the land grid cells can be distributed among available processors based on the estimated workload needed for each of the cells, assuming that computational cost is proportional to the number of sub--grid units. Therefore, the work per processor is roughly the same, and the imbalance resulting from this uneven grid structure is minimized. “*

**Fig. 2:** The degree symbol is missing for the cardinal directions.

A suggested we have now added the degree symbol and units to the map axis wherever needed.

**Fig. 3:** I think I start to understand the splitting of ESM grid cells better but I still struggle to grasp the full details (after looking at Fig. 3 and re-reading Sect. 2.4). I think a reader would understand the splitting better if you illustrate the different stages by means of a single ESM grid cell. The smallest sub-grid units of the cell could then be colour-coded according to the current splitting/clustering stage. I.e. in a first stage, all units would have the same colour. In a second stage, you would have three colours (according to left side, right side and headwaters). And so on...

We agree that this addition would clarify the procedure. We have revised Figure 3 as follows, showing the workflow of our methodology to partition a single grid cell in hillslopes and tiles:



In a first step, based on this set of variables, the land component of the domain is first divided in characteristic hillslope elements. These are obtained by first delineating catchments. A conceptual summary of this clustering procedure is described in Figure 3. The digital elevation map (Figure 3A) is used to compute the drainage network (Figure 3E) necessary to partition the domain in basins (Figure 3B, 3C) based on a threshold area of  $1 \times 10^5 \text{ m}^2$  and by dividing each basin. Basins are in turn subdivided in hillslopes (Figure 3F) following (Chaney et al., 2018): Each basin is divided in up to three contiguous hillslope elements, corresponding to left side, right side, and headwaters.

Then, hillslope elements are aggregated in  $k$  "characteristic hillslopes" via k-means clustering (MacQueen et al., 1967) in the 4-dimensional space of the variables  $\tilde{V}_d$ ,  $\tilde{C}_t$ ,  $S_{sa}$ , and  $C_{sa}$ ; this enables to obtain land units characterized by similar radiation-topography interaction. Figure 3G shows the spatial distribution of these characteristic hillslope clusters for the case  $k = 5$ .

Then, each land unit so obtained. Finally, each of these  $k$  land units is further partitioned into  $p$  sub-units by a second application of the k-means clustering algorithm based on the 4 variables  $\tilde{V}_d$ ,  $\tilde{C}_t$ ,  $S_{sa}$ , and  $C_{sa}$ . A conceptual summary. In figure 3H we show the result of this procedure is described in Figure 3, which yields 25 tiles in this example.